

Supplementary Data

Supplementary methods

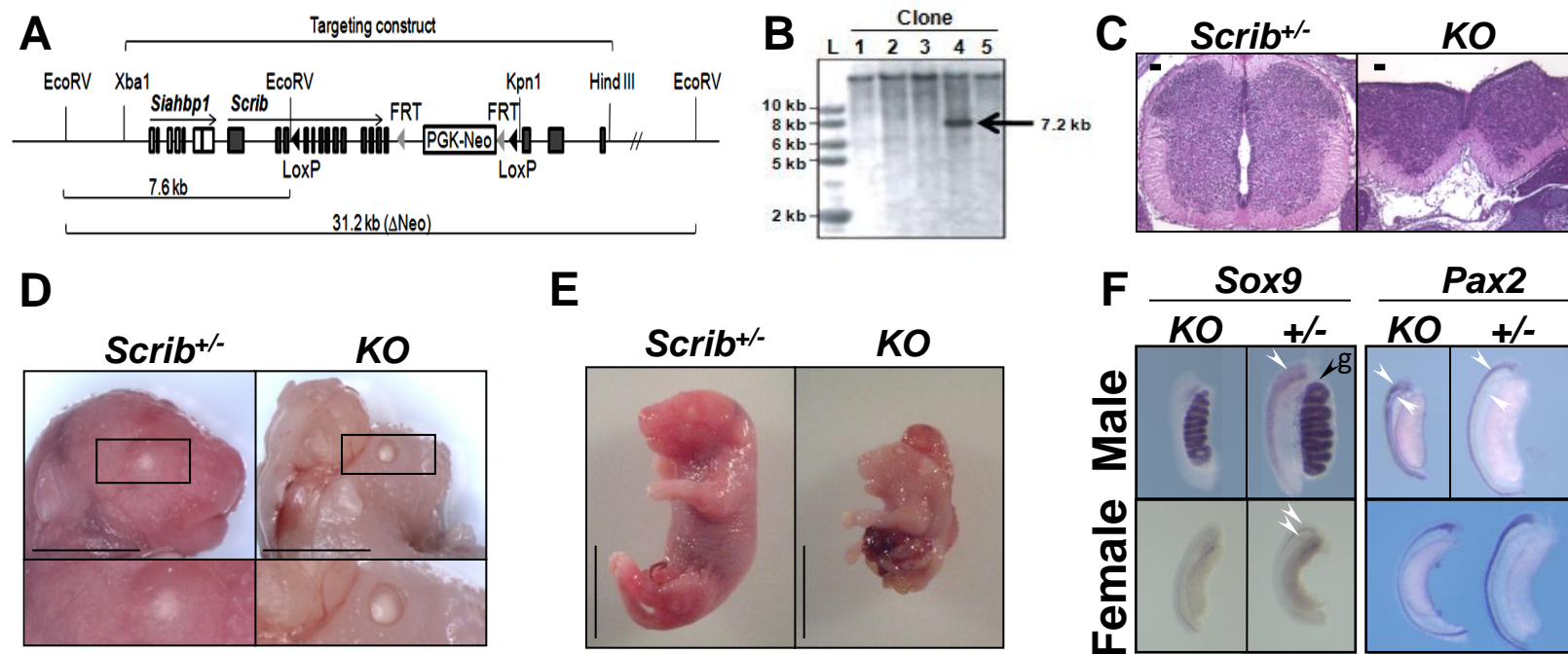
Genotyping. Genotyping to detect WT, floxed and recombined *K-ras* alleles was performed as described previously (1).

Immunohistochemistry and β -gal staining. IHC (FFPE) and β -gal staining were carried out as described previously (2). Primary antibodies include: CK-5 1:1000 (PRB-160P, Covance), CK-8 1:300 (ab-14053 Abcam), Active Caspase-3 1:100 (9664, Cell Signalling Technology) and p-MEK1/2 (Ser221) 1:100 (2338, Cell Signaling Technology). Intensity and cell density scoring was performed using MetaMorph 6.3 software (Molecular Devices) and calculated from the average of three 50 μm^2 regions from a minimum of ten 40x magnification images per mouse (BX-51 Olympus microscope). All analysis was carried out on anterior prostate lobes.

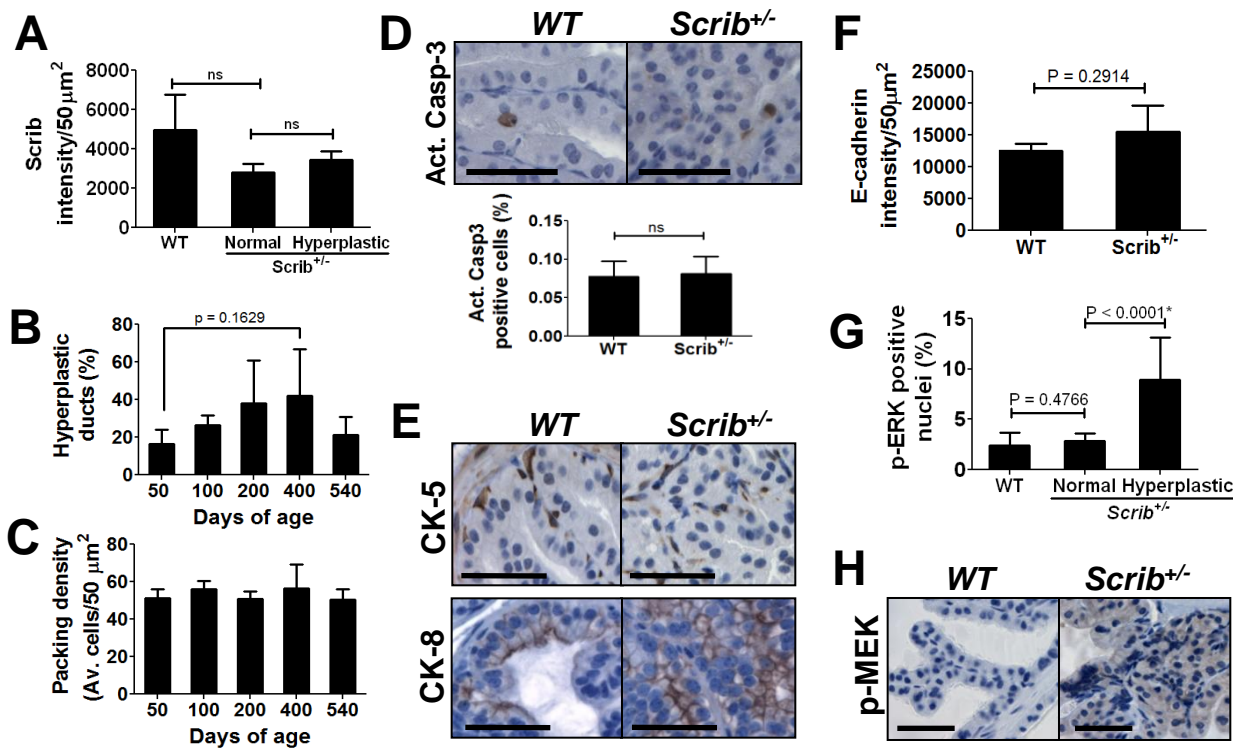
Whole mount in situ hybridisation. E13.5 gonads were harvested and stained for *Pax2* and *Sox9* by *in situ* hybridisation, as described previously (3).

Supplementary References:

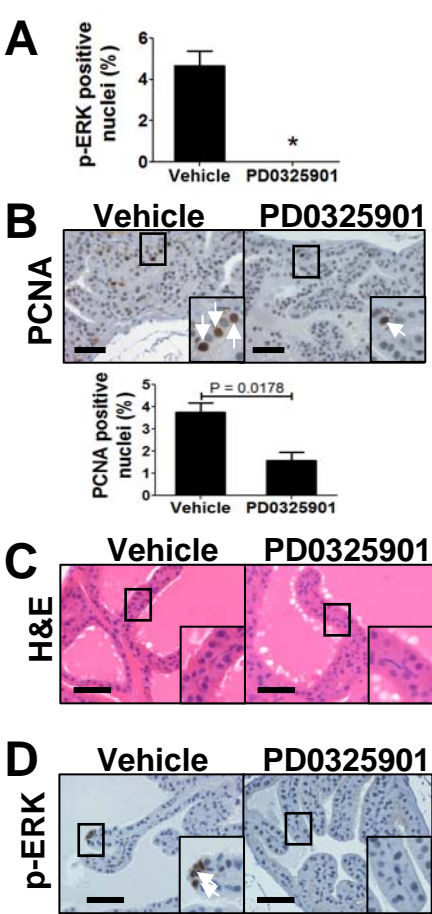
1. Jackson EL, Willis N, Mercer K, Bronson RT, Crowley D, Montoya R, Jacks T, Tuveson DA. 2001. Analysis of lung tumor initiation and progression using conditional expression of oncogenic K-ras. *Genes Dev* 15: 3243-8
2. Pearson H, McCarthy A, Collins C, Ashworth A, Clarke A. 2008. Lkb1 deficiency causes prostate neoplasia in the mouse. *Cancer Res* 68: 1-10
3. Bogani D, Siggers P, Brixey R, Warr N, Beddow S, Edwards J, Williams D, Wilhelm D, Koopman P, Flavell RA, Chi H, Ostrer H, Wells S, Cheeseman M, Greenfield A. 2009. Loss of mitogen-activated protein kinase kinase kinase 4 (MAP3K4) reveals a requirement for MAPK signalling in mouse sex determination. *PLoS Biol* 7: e1000196



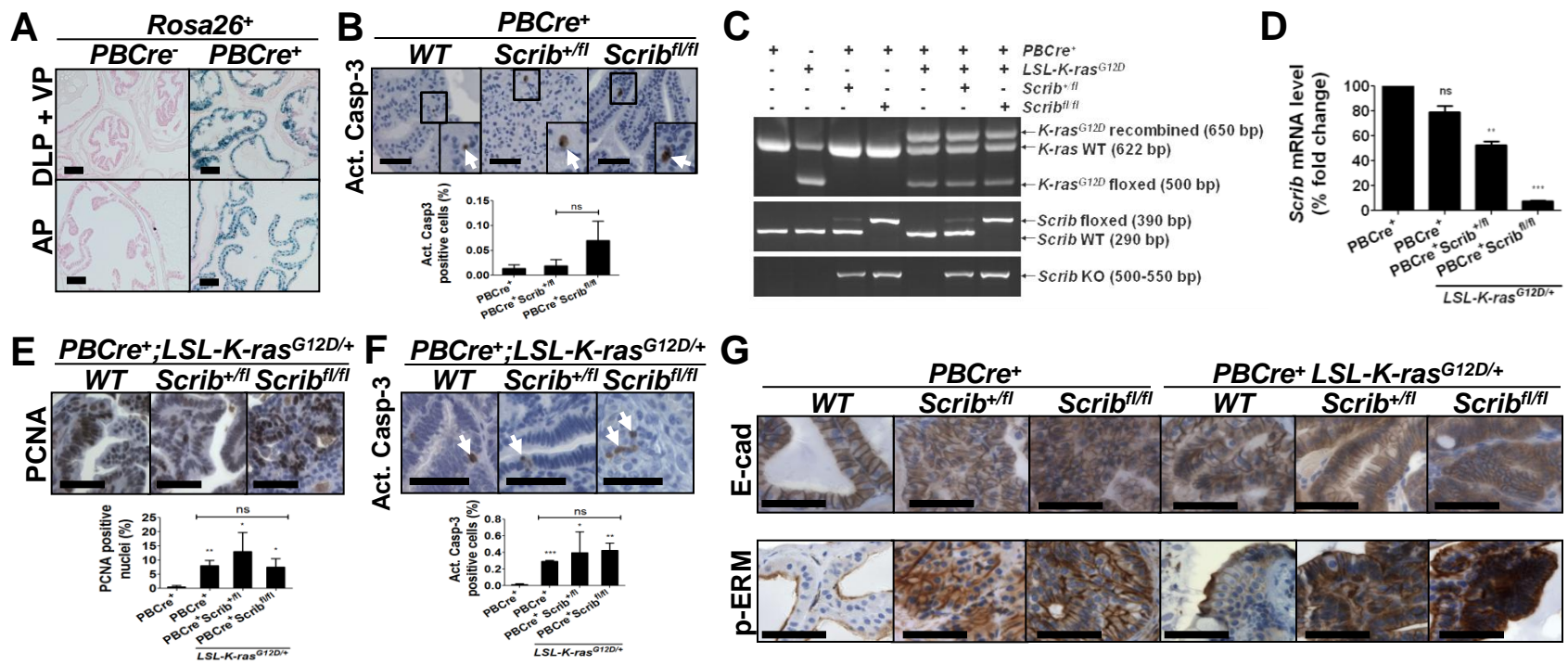
Supplementary Figure 1 Generation and characterisation of *Scrib* *KO* mice. (A) *Scrib* floxed targeting construct. (B) Southern blot analysis of DNA from EcoRV digested ES cell clones (*Scrib^{fl}* = 7.6 kb, *WT* = 31.2 kb). Boxes = exons, triangles = LoxP/FLPe sites. (C) H&E images displaying *Scrib^{KO}* neural tube closure defect and *Scrib^{+/-}* normal closure (E14.5, scale = 50 μ m). (D) *Scrib^{KO}* eyes-open-at-birth phenotype and normal *Scrib^{+/-}* embryos (E18.5, scale = 0.5 cm). (E) *Scrib^{KO}* gasroschisis and normal *Scrib^{+/-}* embryos (E16.5, scale = 1 cm). (F) *In situ* hybridisation to detect the Sertoli marker *Sox9* and *Pax2*, which labels the Müllerian mesenchyme and Müllerian/Wolffian duct epithelia, in male (XY) and female (XX) *Scrib^{+/-}* and *Scrib^{KO}* reproductive organs (E13.5). *Scrib^{KO}* gonads are misshapen and shorter than *Scrib^{+/-}* mice. Male *Scrib^{KO}* gonads exhibit strong *Sox9* expression in the testis cords of the gonad (g), indicating normal primary sex determination. *Scrib^{+/-}* male gonads show normal *Sox9* expression in the Müllerian duct mesenchyme of the mesonephros (white arrowhead) while male *Scrib^{KO}* mesonephros display reduced levels, suggesting reproductive tract development abnormalities. *Scrib^{+/-}* female mesonephros display Müllerian and Wolffian duct epithelia *Sox9* expression (arrowheads), which is depleted in female *Scrib^{KO}* gonads. *Pax2* staining reveals closer proximity of these two ducts in the male *Scrib^{KO}* mesonephros (compare arrowhead positions) and identifies Müllerian duct thinning and reduced staining in the Wolffian duct of the female *Scrib^{KO}* embryos. These abnormalities correspond to those observed in *Crc/Crc* *Scrib* mutants (D.B. and A.G. unpublished observations).



Supplementary Figure 2 Characterisation of *Scrib*^{+/-} prostate hyperplastic lesions. (A) Scoring Scrib IF intensity (shown in Figure 2C) revealed an insignificant reduction in the intensity of Scrib expression in *Scrib*^{+/-} prostate compared to WT tissue ($p \geq 0.1242$, unpaired t-test). (B) The incidence of multifocal hyperplasia in *Scrib*^{+/-} prostate epithelium does not significantly differ with age ($p \geq 0.1629$, unpaired t-test). (C) Packing density of cells per 50 mm^2 region in *Scrib*^{+/-} hyperplastic foci does not alter with age ($p \geq 0.1961$, unpaired t-test). (D) Active Caspase-3 IHC and scoring reveals no alteration in apoptosis in *Scrib*^{+/-} prostate epithelium compared to WT ($p = 0.9097$, unpaired t-test, 400 d). (E) IHC to detect Cytokeratin-5 (CK-5) and Cytokeratin-8 (CK-8) suggests expansion of the CK-8 positive luminal cell population within the *Scrib*^{+/-} hyperplastic lesions, while the CK-5 positive basal population appears unchanged (400 d). (F) Analysis of E-cadherin IHC (shown in Figure 3B) indicates that there is no significant difference in E-cadherin intensity in *Scrib*^{+/-} prostate hyperplasia compared to WT epithelium ($p = 0.2914$, unpaired t-test) at 400 d. (G) p-ERK scoring analysis (shown in figure 3C) reveals no significant difference in p-ERK expression between *Scrib*^{+/-} non-hyperplastic tissue and WT prostate epithelium (unpaired t-test, 400 d). (H) IHC to detect p-MEK revealed an increase in the MAPK signaling cascade in *Scrib*^{+/-} at 400 d, supporting p-ERK staining shown in Figure 3C. Scale bars = 50 μm . Error bars = SD.



Supplementary Figure 3 Characterisation of MEK inhibition in *Scrib*^{+/-} and *WT* prostate epithelium. (A) Analysis of p-ERK IHC (shown in Figure 3E) revealed p-ERK expression is significantly reduced in PD0325901 dosed *Scrib*^{+/-} mice (0% ± 0.000 SD) compared to those receiving vehicle (4.67% ± 1.218 SD, p=0.0220, paired t-test). (B) PCNA IHC and scoring shows a significant reduction in PCNA positive nuclei in *Scrib*^{+/-} mice treated with PD0325901 (1.6% ± 0.63 SD) compared to vehicle (3.8% ± 0.74 SD, p=0.0178, unpaired t-test). (C) H&E images of *WT* prostate administered with vehicle or PD0325901. (D) p-ERK staining to confirm efficient MEK inhibition in *WT* mice administered with vehicle or PD0325901. All mice received PD0325901 (20 mg/kg, 5 d on, 2 d off) for 3 wk or vehicle (aged 230-260 d). Scale bars = 50 μm. Error bars = SD.



Supplementary Figure 4 Characterisation of *Scrib* deficient and *K-ras* activated prostate lesions. (A) LacZ staining *PBCre*⁺;*Rosa26*⁺ prostate lobes confirmed *PBCre*-mediated recombination in all 4 prostate lobes; DLP = dorsolateral, VP = ventral, AP = anterior prostate (400 d). *PBCre*⁻*Rosa26*⁺ control mice were negative for recombination. (B) IHC to detect active Caspase-3 established no significant difference between *PBCre*⁺;*Scrib*^{+fl} and *PBCre*⁺;*Scrib*^{fl/fl} prostates compared to *PBCre*⁺ (p=0.7539 and p=0.2243 respectively, 400 d). (C) PCR analysis of prostate genomic DNA to detect *K-ras* and *Scrib* WT, floxed and recombined alleles. *PBCre*⁺ prostate genomic DNA served as a negative control. (D) qRT-PCR confirmed a significant reduction in *Scrib* mRNA levels in *PBCre*⁺;*Scrib*^{+fl};*LSL-K-ras*^{G12D/+} and *PBCre*⁺;*Scrib*^{fl/fl};*LSL-K-ras*^{G12D/+} prostates compared to *PBCre*⁺ and *PBCre*⁺;*LSL-K-ras*^{G12D/+} prostates (p=0.0370 and p=0.0001 respectively, 400 d). (E) PCNA IHC established a significant increase in PCNA positive cells in *PBCre*⁺;*LSL-K-ras*^{G12D/+} (8.0% ± 1.91 SD), *PBCre*⁺;*Scrib*^{+fl};*LSL-K-ras*^{G12D/+} (13.0% ± 6.72 SD) and *PBCre*⁺;*Scrib*^{fl/fl};*LSL-K-ras*^{G12D/+} (7.5% ± 2.99 SD) prostates compared to WT prostate epithelium (p≤0.0162, 400 d). (F) Active Caspase-3 IHC revealed a significant elevation in apoptotic cells in *PBCre*⁺;*LSL-K-ras*^{G12D/+} (0.3% ± 0.01 SD), *PBCre*⁺;*Scrib*^{+fl};*LSL-K-ras*^{G12D/+} (0.4% ± 0.25 SD) and *PBCre*⁺;*Scrib*^{fl/fl};*LSL-K-ras*^{G12D/+} (0.4% ± 0.09 SD) mutants compared to control mice (0.01% ± 0.01 SD, p ≤ 0.0330, unpaired t-test), yet no statistical difference was apparent when comparing double mutants to *K-ras* activation alone (p>0.5071, unpaired t-test) at 400 d. (G) E-cadherin and p-ERM in *PBCre*⁺, *PBCre*⁺;*Scrib*^{+fl}, *PBCre*⁺;*Scrib*^{fl/fl}, *PBCre*⁺;*LSL-K-ras*^{G12D/+}, *PBCre*⁺;*Scrib*^{+fl};*LSL-K-ras*^{G12D/+} and *PBCre*⁺;*Scrib*^{fl/fl};*LSL-K-ras*^{G12D/+} prostate lesions (400 d). Scale bars = 50 μm. Error bars = SD.

Supplementary Table 1 Clinicopathological features of human prostate TMA.

Characteristic	No. on TMA n=3,261	No. (%) with complete follow-up n=2,891
Follow-up (months)		
Mean		72.1
Median		68.9
Range		0.03-219
Age (years)		
<50	83	78 (94.0)
50-60	998	912 (91.4)
60-70	1,807	1699 (94.0)
>70	175	169 (96.6)
Pre-treatment PSA (ng/ml)		
<4	513	478 (93.2)
4-10	1,673	1544 (92.3)
10-20	641	608 (94.9)
>20	225	212 (94.2)
pT category (AJCC*)		
pT2	2,080	1907 (91.7)
pT3a	609	579 (95.1)
pT3b	372	361 (97.0)
pT4	42	42 (100.0)
Gleason grade		
≤3+3	1,426	1307 (91.7)
3+4	1,311	1238 (94.4)
4+3	313	297 (94.9)
≥4+4	55	49 (89.1)
pN category		
pN0	1,544	1492 (96.6)
pN+	96	93 (96.9)
pNx	1,457	1298 (89.1)
Surgical margin		
Negative	2,475	2295 (92.7)
Positive	627	594 (94.7)

*American Joint Committee on Cancer (2002).

** All categories with absent data, n < 3,261.

Supplementary Table 2 Human prostate TMA SCRIB expression intensity.

Characteristic	n	Neg. (%)	+1 (%)	+2 (%)	+3 (%)	P value**
All Samples	2122	1.5	17.9	34.1	46.5	
Surgical Margin						
Negative	1555	1.4	18.8	34.7	45.1	0.1909
Positive	453	1.5	14.8	34.4	49.2	
Lymph node metastasis						
pN0	1080	1.7	16.4	35.9	46.0	0.8253
pN+	75	1.3	14.7	41.3	42.7	
pT category (AJCC*)						
pT2	1224	1.3	20.7	33.5	44.5	0.0010
pT3a	463	1.9	12.7	34.1	51.2	
pT3b	292	1.0	14.0	41.8	43.2	
pT4	31	0.0	22.6	22.6	54.8	
Gleason grade						
≤3+3	814	1.7	23.8	30.6	43.9	<0.0001
3+4	910	1.2	14.5	37.7	46.6	
4+3	241	1.2	12.4	36.1	50.2	
≥4+4	46	0.0	8.7	41.3	50.0	
Pre-treatment PSA (ng/ml)						
<4	286	1.4	16.1	36.4	46.2	0.0415
4-10	1054	0.8	17.1	32.8	49.3	
10-20	454	2.2	20.0	35.2	42.5	
>20	180	1.7	19.4	41.1	37.8	

*American Joint Committee on Cancer (2002).

**P values represent the χ^2 likelihood test.

Supplementary Table 3 Human prostate TMA SCRIB localisation.

Characteristic	n	Neg. (%)	Normal (%)	Misloc. A (%)	Misloc. B (%)	Misloc. A/B (%)	P value**
All Samples	2122	1.7	91.2	3.4	2.7	1.0	
Surgical Margin							
Negative	1555	1.6	91.8	3.2	2.5	0.9	0.7660
Positive	453	1.8	89.8	4.0	3.3	1.1	
Lymph node metastasis							
pN0	1080	1.8	90.1	4.1	3.1	0.9	0.5866
pN+	75	1.3	85.3	6.7	4.0	2.7	
pT category (AJCC*)							
pT2	1224	1.6	93.5	2.6	1.7	0.6	0.0033
pT3a	463	2.2	89.0	3.9	3.9	1.1	
pT3b	292	1.0	86.3	5.1	5.5	2.1	
pT4	31	0.0	87.1	6.5	3.2	3.2	
Gleason grade							
≤3+3	814	2.3	95.1	1.7	0.4	0.5	<0.0001
3+4	910	1.2	91.2	3.8	2.9	0.9	
4+3	241	1.2	83.0	5.8	7.5	2.5	
≥4+4	46	0.0	69.6	8.7	19.6	2.2	
Pre-treatment PSA (ng/ml)							
<4	286	1.7	90.6	3.1	3.1	1.4	0.0022
4-10	1054	0.9	94.0	2.8	1.6	0.7	
10-20	454	2.4	88.1	4.0	4.0	1.5	
>20	180	2.8	85.0	5.0	6.7	0.6	

*American Joint Committee on Cancer (2002).

**P values represent the χ^2 likelihood test.